ACS OMEGA

Article

Cite This: ACS Omega 2019, 4, 7750−7758

http://pubs.acs.org/journal/acsodf

Quantitative Detection of the Disappearance of the Antioxidant Ability of Catechin by Near-Infrared Absorption and Near-Infrared Photoluminescence Spectra of Single-Walled Carbon Nanotubes

Kazuo Umemura,* Yu Ishibashi, Masahiro Ito, and Yoshikazu Homma

Department of Physics, Tokyo University of Science, 1-3 Kagurazaka, Shinjuku, Tokyo 162-8601, Japan

Supporting Information

ABSTRACT: We succeeded in quantitatively detecting the disappearance of catechin antioxidant ability as a function of time using near-infrared (NIR) absorbance and NIR photoluminescence (PL) spectra of single-walled carbon nanotubes (SWNTs) wrapped with DNA molecules (DNA−SWNT hybrids). When 15 μg/mL of catechin was added to the oxidized hybrid suspension, the absorbance of SWNTs increased, according to the antioxidant ability of catechin, and the effect was maintained at least for 30 min. When catechin concentrations were less than 0.3 μg/mL, SWNT absorbance gradually decreased, although it increased when catechin is added. The results revealed that disappearance of the catechin effects could be quantitatively detected by NIR absorbance spectra. When NIR PL was employed, the disappearance of PL intensity was also observed in the case of low catechin concentrations. However, time-lapse measurement of the disappearance was difficult because the PL intensity was rapidly quenched. In addition, the optical responses were different due to different chirality of SWNTs. Our results suggested that both NIR absorbance and PL can detect disappearance of catechin antioxidant effects; in particular, slow response of NIR absorbance was effective to detect time dependence of the disappearance of the catechin effects. Contrarily, PL revealed huge and rapid responses in contrast to NIR absorbance. PL might be effective for reversible use of DNA−SWNT hybrids as a nanobiosensor.

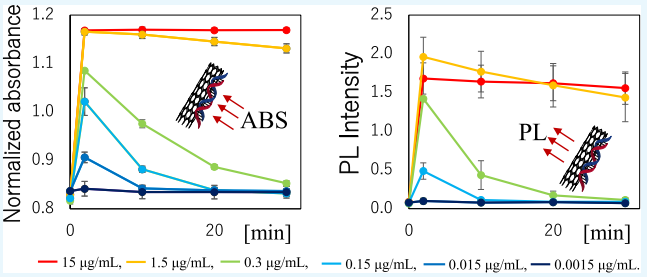

INTRODUCTION

Near-infrared (NIR) absorption spectra of single-walled carbon nanotubes (SWNTs) are sensitive against structural and physicochemical changes of SWNTs.[1−3] For example, it is known that NIR absorbance is weakened when SWNTs are oxidized.[4] NIR photoluminescence (PL) from SWNTs by irradiation with visible lights is also fluctuated according to structures of SWNTs and changes of sample conditions.[5−18] These unique optical responses of SWNTs can therefore be applied to various biological applications.[19−27] Especially, nanobiosensing that uses SWNT unique optical properties is one of the promising approaches, and attachment of biomolecules onto DNA−SWNTs to functionalize the hybrids has been intensively studied by many research groups.[28−39]

For example, Zhao et al. proposed an impressive strategy for nanobiosensing in 2015.[40] First, DNA-wrapped SWNT suspensions (DNA−SWNT hybrids) were prepared as usual. In their study, DNA was only used to solubilize SWNTs. Second, hydrogen peroxide (H_2O_2), hydroxyl radicals, caffeine, regular coffee, and decaffeinated coffee were added to the DNA−SWNT suspension. They found that a specific peak of NIR absorption spectra that originated from (10, 5) SWNTs of the DNA−SWNT hybrids significantly decreased in the presence of oxidants such as H_2O_2 or hydroxyl radicals. (10, 5) defines the chirality of a specific SWNT that is sensitive to oxidation/reduction. In contrast, in the presence of reductants such as coffee and caffeine, the NIR peaks were significantly recovered.

Strano's group published many papers of biological sensing using SNNTs. Especially, chirality effects on PL spectra were one of their recent targets.[41−46] Xu et al. studied effect of H_2O_2, glucose, and glucose oxidase (GOx) on NIR absorbance of DNA−SWNT hybrids.[4] Tu et al. also reported changes in NIR absorbance with H_2O_2 addition under various pH conditions.[47] Kurnosov et al. studied effects of cysteine on DNA−SWNT hybrids and other related important biological molecules.[38] Kruss et al. employed hybrids of polymers and SWNTs including DNA; Polo et al. covered SWNTs with various polymers and found DNA and other polymers behave in different manner.[31,48,49] Nanobiosensing using SWNTs became an attractive research subject.[50−52]

We reported detection of antioxidant effects of Japanese tea and catechin using both NIR absorption spectra and NIR PL spectra.[53] Catechin is one of the major components of Japanese tea. We found that the effects can be well detected by both of the spectra. In particular, change of PL spectra was much drastic than that of NIR absorbance spectra. However,

Received: March 20, 2019
Accepted: April 18, 2019
Published: April 29, 2019

DOI: 10.1021/acsomega.9b00767
ACS Omega 2019, 4, 7750−7758

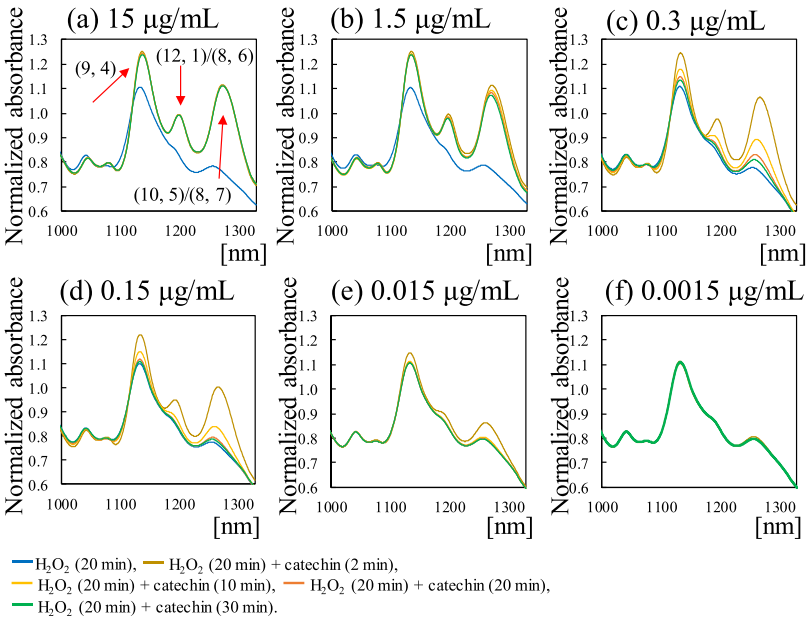

Figure 1. NIR absorbance spectra of DNA–SWNT hybrids in the presence or absence of catechin. Catechin concentration ranged from 0 to 15 μg/mL. (a) 15, (b) 1.5, (c) 0.3, (d) 0.15, (e) 0.015, and (f) 0.0015 μg/mL. Blue line: DNA–SWNTs oxidized with 0.03% H_2O_2 solution for 20 min. Then, the oxidized DNA–SWNTs were incubated with catechin for 2 min (gold line), 10 min (yellow line), 20 min (orange line), and 30 min (green line). The arrow indicates the peak of (10, 5)/(8, 7) SWNTs. The absorbance values represent the mean of three independent measurements.

concentrations of catechin and tea were fixed at 15 μg/mL in that report.

In this study, we detected the disappearance of antioxidant properties of catechin when low concentrations of catechin solutions were employed. Variously diluted catechin solutions were added to DNA–SWNT hybrids, and reduction of SWNTs was evaluated by analysis of NIR absorption and NIR PL spectra. Although stable recovery of NIR peaks was observed with 15 μg/mL of catechin as we reported previously, recovered NIR peaks decreased again as a function of time with diluted catechin solutions.

RESULTS AND DISCUSSION

Figure 1 shows the NIR absorbance spectra of DNA–SWNT hybrids before and after incubating with various concentrations of catechin. The hybrids were first oxidized with H_2O_2 (final concentration 0.03%) for 20 min, and the catechin solution was then injected. The blue line in Figure 1 indicates the absorbance in the absence of catechin and, therefore, the absorbance of oxidized SWNTs. Then, various concentrations of catechin solutions were added to the samples, and then, NIR absorbance spectra were measured after 2 min (gold line), 10 min (yellow line), 20 min (orange line), and 30 min (green line). As a result, a peak around 1260 nm that was E11 of (10, 5)/(8, 7) SWNTs revealed clear responses (see the arrow in Figure 1a).[54,55] When the final concentration of catechin was 15 μg/mL, the absorbance increased 143.6% after 2 min against that of oxidized samples. We also continuously measured time dependence of NIR absorbance spectra only with H_2O_2 as shown in Figure S1.

Numerical values are shown in Table 1. If the initial absorbance of (10, 5)/(8, 7) was defined as 100%, the absorbance value after 20 min incubation with H_2O_2 was 81.3% in the case of 15 μg/mL of catechin. The value after incubation for 2 min with catechin was 116.7%. It is clear that NIR absorbance of (10, 5)/(8, 7) was decreased with H_2O_2 and recovered with catechin. Even after incubating for 30 min with catechin, the absorbance peak did not decrease again. Thus, gold, yellow, orange, and green lines were completely overlapped in Figure 1a. It suggests that antioxidant effects of 15 μg/mL of catechin were enough strong at least for 30 min.

When the catechin concentration was 1.5 μg/mL, the peak slightly decreased after 30 min (Figure 1b). Based on the numerical analysis in Table 1, the value increased to 102.4 and 113.1% for (9, 4) and (10, 5)/(8, 7), respectively, against that of the initial suspension when the sample was incubated with catechin for 2 min. However, after 30 min incubation, it was 109.1%. This decrease was more clearly observed when 0.3 μg/mL of catechin was added to the sample (Figure 1c). The peak around 1260 nm gradually decreased due to incubation. The data suggest that 0.3 μg/mL of catechin was enough to recover the absorbance spectra of DNA–SWNTs once; however, the recovery effects were limited. The effects of catechin were gradually weakened due to concentrations of catechin (Figure 1c–f). After all, when 0.0015 μg/mL of catechin was used, significant recovery was not observed even in 2 min incubation (Figure 1f). From the numerical analysis in Table 1, when the catechin concentrations were 0.15 and 0.015 μg/mL for 2 min incubation, recovery ratios in (10, 5)/(8, 7) were 99.0 and 86.9%, respectively, and those in (9, 4) and (10, 5)/(8, 7) were 99.2 and 94.3%, respectively. Although the absorbance values were increased compared to those with H_2O_2, the values were reached to the initial state (without H_2O_2 and catechin). Although the mechanism of this decrease is not clear at this moment, as one possibility, H_2O_2 or O_2 in the sample was competitive against catechin.

Figure 2 shows NIR PL spectra of similar samples before and after incubating with various concentrations of catechin. NIR PL spectra only with H_2O_2 are shown in Figure S2. Excitation wavelength was 730 nm in Figures 2 and S2. NIR PL spectra with excitation wavelength 740 nm are shown in

DOI: 10.1021/acsomega.9b00767
ACS Omega 2019, 4, 7750–7758

Table 1. Numerical Analysis of NIR Absorbance Spectra

catechin concentration [mg/mL]		initial		H_2O_2, 2 min		H_2O_2, 20 min		catechin, 2 min		catechin, 10 min		catechin, 20 min		catechin, 30 min	
15	(9, 4)	1.22 ± 0.00 (1134)	100.0	1.15 ± 0.01 (1133)	94.3	1.12 ± 0.01 (1133)	91.8	1.25 ± 0.01(1136)	102.5	1.25 ± 0.01 (1136)	102.5	1.25 ± 0.01(1136)	102.5	1.25 ± 0.01 (1137)	102.5
	(10, 5)/ (8, 7)	0.96 ± 0.00 (1265)	100.0	0.85 ± 0.01 (1261)	88.5	0.78 ± 0.00 (1256)	81.3	1.12 ± 0.00(1272)	116.7	1.12 ± 0.01 (1272)	116.7	1.12 ± 0.01(1273)	116.7	1.12 ± 0.01 (1273)	116.7
1.5	(9, 4)	1.23 ± 0.01 (1134)	100.0	1.15 ± 0.01 (1133)	93.5	1.11 ± 0.01 (1133)	90.2	1.26 ± 0.01(1134)	102.4	1.25 ± 0.01 (1135)	101.6	1.25 ± 0.01(1134)	101.6	1.25 ± 0.01 (1134)	101.6
	(10, 5)/ (8, 7)	0.99 ± 0.01 (1266)	100.0	0.86 ± 0.00 (1261)	86.9	0.78 ± 0.01 (1256)	78.8	1.12 ± 0.01(1271)	113.1	1.11 ± 0.01 (1271)	112.1	1.10 ± 0.01(1269)	111.1	1.08 ± 0.01 (1269)	109.1
0.3	(9, 4)	1.19 ± 0.02 (1134)	100.0	1.13 ± 0.01 (1133)	95.0	1.10 ± 0.00 (1132)	92.4	1.24 ± 0.00(1134)	104.2	1.20 ± 0.01 (1134)	100.8	1.15 ± 0.00(1133)	96.6	1.13 ± 0.00 (1133)	95.0
	(10, 5)/ (8, 7)	0.88 ± 0.04 (1263)	100.0	0.82 ± 0.03 (1260)	93.2	0.77 ± 0.01 (1254)	87.5	1.05 ± 0.01(1268)	119.3	0.93 ± 0.02 (1264)	105.7	0.84 ± 0.01(1262)	95.5	0.80 ± 0.01 (1259)	90.9
0.15	(9, 4)	1.23 ± 0.01 (1134)	100.0	1.14 ± 0.01 (1133)	92.7	1.11 ± 0.01 (1133)	90.2	1.22 ± 0.01(1134)	99.2	1.15 ± 0.00 (1133)	93.5	1.13 ± 0.01(1133)	91.9	1.12 ± 0.01 (1133)	91.1
	(10, 5)/ (8, 7)	0.98 ± 0.00 (1266)	100.0	0.84 ± 0.00 (1260)	85.7	0.77 ± 0.00 (1257)	78.6	0.97 ± 0.03(1266)	99.0	0.83 ± 00.01 (1260)	84.7	0.79 ± 0.01(1258)	80.6	0.78 ± 0.01 (1257)	79.6
0.015	(9, 4)	1.22 ± 0.00 (1134)	100.0	1.14 ± 0.01 (1133)	93.4	1.10 ± 0.01 (1134)	90.2	1.15 ± 0.00(1134)	94.3	1.11 ± 0.00 (1133)	91.0	1.10 ± 0.00(1134)	90.2	1.10 ± 0.01 (1133)	90.2
	(10, 5)/ (8, 7)	0.99 ± 0.01 (1266)	100.0	0.85 ± 0.02 (1261)	85.9	0.79 ± 0.01 (1255)	79.8	0.86 ± 0.01(1261)	86.9	0.79 ± 0.01 (1257)	79.8	0.79 ± 0.01(1257)	79.8	0.79 ± 0.01 (1254)	79.8
0.0015	(9, 4)	1.23 ± 0.01 (1134)	100.0	1.15 ± 0.01 (1133)	93.5	1.11 ± 0.00 (1133)	90.2	1.12 ± 0.00(1133)	91.1	1.11 ± 0.00 (1133)	90.2	1.11 ± 0.00(1133)	90.2	1.11 ± 0.00 (1133)	90.2
	(10, 5)/ (8, 7)	1.00 ± 0.01 (1266)	100.0	0.87 ± 0.01 (1262)	87.0	0.79 ± 0.01 (1256)	79.0	0.79 ± 0.02(1257)	79.0	0.78 ± 0.01 (1257)	78.0	0.78 ± 0.01(1257)	78.0	0.78 ± 0.01 (1257)	78.0

DOI: 10.1021/acsomega.9b00767
ACS Omega 2019, 4, 7750−7758

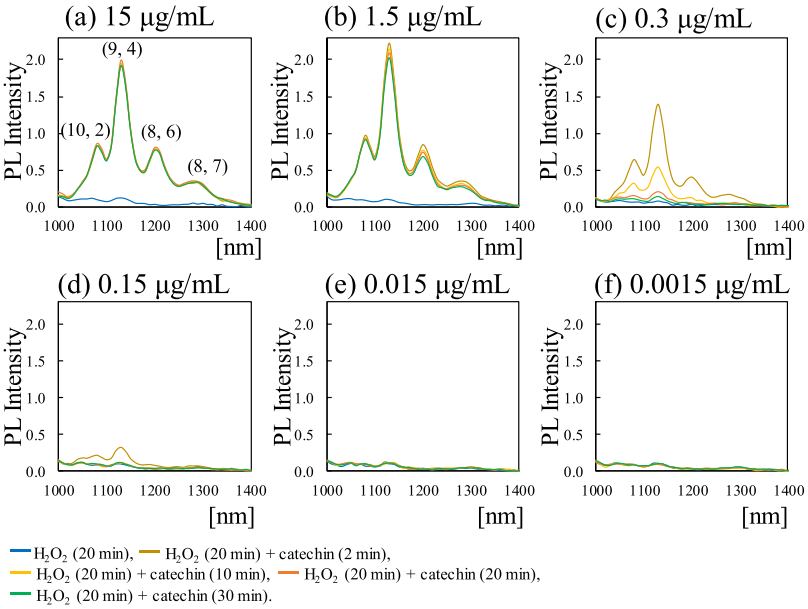

Figure 2. NIR PL spectra of DNA–SWNT hybrids in the presence or absence of catechin. Excitation wavelength was 730 nm. Catechin concentration ranged from 0 to 15 μg/mL. (a) 15, (b) 1.5, (c) 0.3, (d) 0.15, (e) 0.015, and (f) 0.0015 μg/mL. Blue line: DNA–SWNTs oxidized with 0.03% H_2O_2 solution for 20 min. Then, the oxidized DNA–SWNTs were incubated with catechin for 2 min (gold line), 10 min (yellow line), 20 min (orange line), and 30 min (green line). The arrow indicates the peak of (9, 4) SWNTs. The absorbance values represent the mean of three independent measurements.

Figure S3. PL maps of related samples were studied in our previous paper, and we found that several clear PL spots were obtained by 730 nm excitation.[53] For this reason, we focused on excitation at 730 and 740 nm in this paper. By focusing on the narrow range of the excitation wavelengths, time-lapse measurements were available although it takes time to obtain PL maps. Numerical analysis for 730 and 740 nm excitation is shown in Tables 2 and S2, respectively. PL intensity increased 446.7% against that of initial suspension in the case of (8, 6) SWNTs when 15 μg/mL of catechin was added (see the arrow in Figure 2a). Comparing with oxidized SWNTs with 20 min incubation with H_2O_2, it was a 3350.0% increase. As we reported in our previous paper, PL sensitivity was much higher than that of NIR absorbance.[53] In the case of PL, luminous efficiency is affected by electron density. Thus, the efficiency should be decreased when SWNTs are oxidized. This might be one of the reasons of high recovery in PL.[56−63]

In addition, PL recovery of (8, 6) is larger than that of (9, 4), (8, 7), and (10, 2). For example, recovery ratios of (8, 6) with 15, 1.5, and 0.3 μg/mL of catechin for 2 min incubation were 446.7, 423.5, and 330.8%, respectively; those of (9, 4) with 15, 1.5, and 0.3 μg/mL of catechin for 2 min incubation were 250.7, 264.9, and 240.7%, respectively; those of (8, 7) with 15, 1.5, and 0.3 μg/mL of catechin for 2 min incubation were 400.0, 362.5, and 250.0%, respectively; and those of (10, 2) with 15, 1.5, and 0.3 μg/mL of catechin for 2 min incubation were 190.7, 201.7, and 189.4%, respectively. It is known that diameters of (9, 4), (8, 6), (8, 7), and (10, 2) are 0.916, 0.966, 1.032, and 0.884 nm, respectively.[17] The PL data roughly suggested that thin SWNTs are more sensitive although the order of (9, 4) and (8, 6) is not reasonable.

When diluted catechin solution was used, limitation of catechin effects also appeared in PL spectra as well as in absorbance spectra. For example, in the case of 0.3 μg/mL of catechin, PL intensity of (8, 6) increased 330.8% against the initial suspension for 2 min incubation with catechin. However, the values were 100.0, 30.8, and 23.1% for 10, 20, and 30 min incubation with catechin. A similar decrease according to incubation time was observed in (9, 4), (8, 7), and (10, 2) when the catechin concentrations were less than 0.3 μg/mL.

Interestingly, NIR absorbance had longer lifetime than PL when diluted catechin solution was employed. We can compare the results about (9, 4) because (9, 4) was measured in both absorbance and PL. In the case of 0.15 μg/mL of catechin, NIR absorbance values were 90.2, 99.2, 93.5, 91.9, and 91.1% against the initial suspension for 20 min incubation with H_2O_2, 2 min with catechin, 10 min with catechin, 20 min with catechin, and 30 min with catechin, respectively. On the other hand, PL intensities were 10.5, 64.5, 14.5, 11.8, and 11.8% against the initial suspension for 20 min incubation with H_2O_2, 2 min with catechin, 10 min with catechin, 20 min with catechin, and 30 min with catechin, respectively. Recovery of NIR absorbance continued at least for 30 min although the values were gradually decreased. Instead, PL intensity dramatically decreased after 10 min incubation with catechin (14.5%), although there was a significant recovery for 2 min incubation (64.5%).

Comparison of NIR absorbance of (10, 5)/(8, 7) and PL of (8, 7) at 0.15 μg/mL of catechin provides more clear difference. In NIR absorbance, values were 78.6, 99.0, 84.7, 80.6, and 79.6% against the initial suspension for 20 min incubation with H_2O_2, 2 min with catechin, 10 min with catechin, 20 min with catechin, and 30 min with catechin, respectively. PL intensities were 50.0, 87.5, 50.0, 50.0, and 50.0% against the initial suspension for 20 min incubation with H_2O_2, 2 min with catechin, 10 min with catechin, 20 min with catechin, and 30 min with catechin, respectively. In this case, NIR absorbance of (10, 5)/(8, 7) well detected the time-lapse decrease; however, PL was not suitable to detect time dependence because the decrease was too fast. As we discussed the above, PL intensity of oxidized SWNTs is strongly inhibited due to the decrease of density of electric states. It

DOI: 10.1021/acsomega.9b00767
ACS Omega 2019, 4, 7750−7758

Table 2. Numerical Analysis of NIR PL Spectra[a]

catechin concentration [mg/mL]		initial		H_2O_2, 2 min		H_2O_2, 20 min		catechin, 2 min		catechin, 10 min		catechin, 20 min		catechin, 30 min	
15	(9, 4)	0.67 ± 0.10	100.0	0.14 ± 0.03	20.9	0.09 ± 0.02	13.4	1.68 ± 0.20	250.7	1.64 ± 0.21	244.8	1.62 ± 0.23	241.8	1.56 ± 0.21	232.8
	(8, 6)	0.15 ± 0.02	100.0	0.03 ± 0.01	20.0	0.02 ± 0.01	13.3	0.67 ± 0.09	446.7	0.66 ± 0.09	440.0	0.65 ± 0.10	433.3	0.63 ± 0.09	420.0
	(8, 7)	0.07 ± 0.01	100.0	0.04 ± 0.01	57.1	0.04 ± 0.00	57.1	0.28 ± 0.04	400.0	0.29 ± 0.03	414.3	0.28 ± 0.04	400.0	0.27 ± 0.04	385.7
1.5	(9, 4)	0.74 ± 0.15	100.0	0.14 ± 0.04	18.9	0.08 ± 0.01	10.8	1.96 ± 0.25	264.9	1.77 ± 0.26	239.2	1.59 ± 0.28	214.9	1.44 ± 0.31	194.6
	(8, 6)	0.17 ± 0.04	100.0	0.03 ± 0.01	17.6	0.03 ± 0.01	17.6	0.72 ± 0.11	423.5	0.60 ± 0.11	352.9	0.51 ± 0.12	300.0	0.44 ± 0.12	258.8
	(8, 7)	0.08 ± 0.01	100.0	0.04 ± 0.01	50.0	0.04 ± 0.00	50.0	0.29 ± 0.04	362.5	0.23 ± 0.04	287.5	0.19 ± 0.05	237.5	0.16 ± 0.04	200.0
0.3	(9, 4)	0.59 ± 0.03	100.0	0.11 ± 0.01	18.6	0.07 ± 0.00	11.9	1.42 ± 0.01	240.7	0.59 ± 0.04	100.0	0.22 ± 0.01	37.3	0.14 ± 0.01	23.7
	(8, 6)	0.13 ± 0.01	100.0	0.03 ± 0.00	23.1	0.02 ± 0.01	15.4	0.43 ± 0.01	330.8	0.13 ± 0.01	100.0	0.04 ± 0.00	30.8	0.03 ± 0.01	23.1
	(8, 7)	0.06 ± 0.00	100.0	0.04 ± 0.00	66.7	0.04 ± 0.00	66.7	0.15 ± 0.00	250.0	0.06 ± 0.01	100.0	0.05 ± 0.00	83.3	0.04 ± 0.01	66.7
0.15	(9, 4)	0.76 ± 0.18	100.0	0.14 ± 0.04	18.4	0.08 ± 0.02	10.5	0.49 ± 0.11	64.5	0.11 ± 0.00	14.5	0.09 ± 0.01	11.8	0.09 ± 0.01	11.8
	(8, 6)	0.18 ± 0.05	100.0	0.03 ± 0.01	16.7	0.03 ± 0.00	16.7	0.11 ± 0.03	61.1	0.03 ± 0.01	16.7	0.02±0.01	11.1	0.03 ± 0.00	16.7
	(8, 7)	0.08 ± 0.02	100.0	0.05 ± 0.01	62.5	0.04 ± 0.01	50.0	0.07 ± 0.00	87.5	0.04 ± 0.01	50.0	0.04 ± 0.01	50.0	0.04 ± 0.00	50.0
0.015	(9, 4)	0.69 ± 0.15	100.0	0.15 ± 0.05	21.7	0.08 ± 0.02	11.6	0.11 ± 0.04	15.9	0.08 ± 0.04	11.6	0.08 ± 0.02	11.6	0.07 ± 0.02	10.1
	(8, 6)	0.16 ± 0.03	100.0	0.04 ± 0.01	25.0	0.03 ± 0.01	18.8	0.03 ± 0.01	18.8	0.02 ± 0.01	12.5	0.02 ± 0.01	12.5	0.02 ± 0.01	12.5
	(8, 7)	0.07 ± 0.01	100.0	0.04 ± 0.01	57.1	0.04 ± 0.00	57.1	0.04 ± 0.01	57.1	0.04 ± 0.01	57.1	0.04 ± 0.01	57.1	0.04 ± 0.01	57.1
0.0015	(9, 4)	0.84 ± 0.03	100.0	0.18 ± 0.04	21.4	0.10 ± 0.02	11.9	0.11 ± 0.03	13.1	0.10 ± 0.02	11.9	0.09 ± 0.02	10.7	0.09 ± 0.02	10.7
	(8, 6)	0.19 ± 0.01	100.0	0.05 ± 0.01	26.3	0.03 ± 0.00	15.8	0.03 ± 0.00	15.8	0.03 ± 0.00	15.8	0.02 ± 0.01	10.5	0.02 ± 0.01	10.5
	(8, 7)	0.08 ± 0.01	100.0	0.04 ± 0.01	62.5	0.05 ± 0.00	62.5	0.04 ± 0.00	50.0	0.05 ± 0.01	62.5	0.04 ± 0.00	50.0	0.05 ± 0.00	62.5

[a]Excitation wavelength was 730 nm.

DOI: 10.1021/acsomega.9b00767
ACS Omega 2019, 4, 7750−7758

might be one of the reasons of low sensitivity of PL monitoring when catechin concentrations were low.

Figure 3 shows summary of time dependence of the NIR absorbance ((10, 5)/(8, 7) SWNTs) and NIR PL ((9, 4) SWNTs). These chiralities were selected to indicate the best performance of absorbance and PL methods. In the NIR absorbance, absorbance values were stable even after 30 min incubation when 15 μg/mL of catechin was employed. Even with 1.5 μg/mL, decrease of absorbance values was not huge. Contrarily, in the case of PL intensity, even with 15 and 1.5 μg/mL of catechin, the PL intensity gradually decreased during 30 min incubation. When diluted catechin solutions (0.015 and 0.0015 μg/mL of catechin) were used, it was hard to monitor time dependence of intensity values. In summary, when catechin concentration was high (15 μg/mL), PL spectra was suitable to detect the catechin effects clearly. Contrarily, when the catechin concentration was low (less than 0.15 μg/mL), NIR absorbance was suitable to well detect the time dependence of catechin effects.

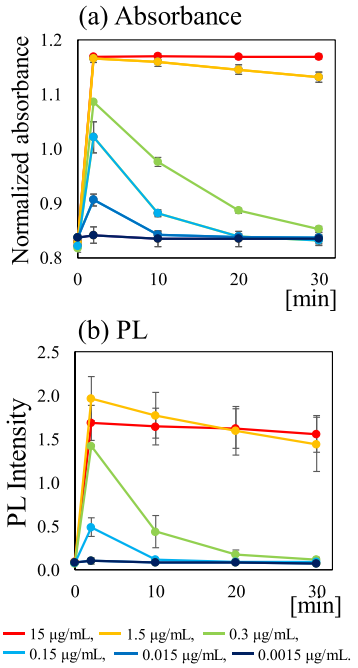

Figure 3. Time dependence of (a) NIR absorbance values of (10, 5)/(8, 7) SWNTs and (b) NIR PL intensities of (9, 4) SWNTs. The value at 0 min reveals the values before adding catechin. After adding catechin, the values were measured after incubation 2, 10, 20, and 30 min. Catechin concentrations were 15 μg/mL (red line), 1.5 μg/mL (yellow line), 0.3 μg/mL (green line), 0.15 μg/mL (sky blue line), 0.015 μg/mL (dark blue line), and 0.0015 μg/mL (black line).

Several discussions are available based on the above experimental results. First, our results suggest that spectral change of SWNTs caused by catechin was reversible because the catechin effects disappeared as a function of time with diluted catechin solutions. If structures or physicochemical properties of SWNTs were permanently changed by catechin, the catechin effect should be continued for longer time. This is one of the important points for biosensing applications of SWNTs because it suggests that reversible use of DNA–SWNT hybrids is available. There are many future research themes in near future. For example, detailed evaluation of reversibility of time-lapse measurement is necessary. Interactions among catechin, DNA, and H_2O_2 will be evaluated.

Second, the speed of disappearance of catechin effects is much faster in PL in contrast to that in absorbance. Probably, the mechanism to produce PL is more complicated than absorbance; thus, PL might be easily disappeared. But the reason of this difference is not easy to explain. For practical viewpoint, it looks that both PL and absorbance have different advantages. Rapid response of PL is suitable to expect reversible use of DNA–SWNT hybrids for nanobiosensing. It is not necessary to wait a long time to start the second measurements. In contrast, for analysis of relaxation process of SWNT spectra, absorbance has advantages over PL because absorbance peaks gradually decreased.

Third, redox potentials of each molecule are probably important factors to understand the observed phenomena.[64−66] Reduction potential of H_2O_2 is around 1.7 V and that of catechin is less than 0.1 V. Although reduction potential of SWNTs is varied due to their chiralities, it is much higher than those of catechin and H_2O_2. For example, the potential of (9, 4) was reported to be around 4 V. The difference of the potentials is reasonable to explain our spectral data.

In summary, our data revealed disappearance of catechin effects by both absorbance and PL for the first time. This provides helpful information to establish nanobiosensing technology using DNA–SWNT hybrids.

CONCLUSIONS

We demonstrated quantitative detection of disappearance of antioxidant effects of catechin using DNA–SWNT hybrids in an aqueous solution. We found that both NIR absorbance spectra and PL spectra could detect the disappearance of the effects when the catechin concentration was less than 0.3 μg/mL. On the other hand, quenching speed of PL intensity was much faster than NIR absorbance. The slow response of NIR absorbance was useful for time-lapse measurements of the disappearance of the catechin effects. Our results indicated a potential of time-lapse nanobiosensing using DNA–SWNT hybrids.

MATERIALS AND METHODS

SWNTs produced by the high-pressure carbon monooxide (HiPco) method were obtained from Unidym Inc. (Sunnyvale, CA, USA). Deoxyribonucleic acid sodium salt from salmon testes (D1626, dsDNA) was bought from Sigma-Aldrich Co. (St. Louis, MO, USA). H_2O_2 (abt. 30%, 084-07441) and epigallocatechin gallate (553-74471, catechin) were purchased from Wako Pure Chemical Industries, Ltd. (Osaka, Japan).

DNA was dissolved in 10 mM tris(hydroxymethyl)-aminomethane (Tris-HCl buffer solution, pH 7.3). DNA concentration was 1 mg/mL. To prepare a uniform DNA solution, it was sonicated in an ultrasonic bath (80 W) for 90 min on ice. Finally, the DNA solution was gently shaken for 3 h. Catechin was dissolved in pure water (1.5 mg/mL) and stored after gentle shaking.

SWNT (powder, 0.5 mg) and DNA solution (1 mL, pH 7.3) were mixed and sonicated for 2 h using a probe-type sonicator (3 W) on ice.[53] The supernatant was stored as the DNA–SWNT suspension after centrifugation at 15 000 rpm (17 360g) for 3 h at 8 °C.

NIR absorption spectra were measured by SolidSpec-3700DUV (Shimadzu Co., Kyoto, Japan). NIR PL spectra

DOI: 10.1021/acsomega.9b00767
ACS Omega 2019, 4, 7750−7758

were obtained by NIR-PL System (Shimadzu Co., Kyoto, Japan). Measurement procedures were similar in both absorbance and PL spectroscopy. DNA−SWNT suspension (50 μL) and Tris-HCl buffer solution (930 μL) were mixed in a sample tube and deaerated by nitrogen gas. The NIR spectrum of the mixture was measured in a quartz cuvette with sealing. After measuring the initial spectra, H_2O_2 solution was added to the mixture (final concentration 0.03%, 8.8 mM), and NIR spectra were then measured after 2 and 20 min of incubation at 21 °C. Finally, 10 μL of the catechin solution was added to the samples (the final concentration was 15, 1.5, 0.3, 0.15, 0.015, or 0.0015 μg/mL), and the spectra were measured again after 2, 10, 20, and 30 min of incubation at 21 °C. Molar concentrations of catechin were 33, 3.3, 0.33, 0.033, and 0.0033 μM. Molar concentration of H_2O_2 was much higher than that of catechin. Each experiment was repeated three times to verify the reproducibility. The obtained NIR spectra were normalized to an adsorption wavelength of 730.5−732.25 nm (E22 of (9, 4)). Assignments of chirality of each SWNT were carried out based on several previous papers.[54,55]

■ ASSOCIATED CONTENT

Supporting Information

The Supporting Information is available free of charge on the ACS Publications website at DOI: 10.1021/acsomega.9b00767.

NIR absorbance spectra of DNA−SWNT hybrids in the presence or absence of H_2O_2 and catechin; NIR PL spectra of DNA−SWNT hybrids in the presence or absence of catechin; NIR PL spectra of DNA−SWNT hybrids in the presence or absence of catechin; and numerical analysis of NIR PL spectra (excitation wavelength: 740 nm) (PDF)

■ AUTHOR INFORMATION

Corresponding Author

*E-mail: meicun2006@163.com. Phone: +81-352288228.

ORCID

Kazuo Umemura: 0000-0002-8073-3903

Author Contributions

K.U. and Y.I. contributed equally to the work. K.U. designed the study, analyzed the experimental data, and drafted the manuscript. Y.I. carried out the experiments including sample preparations, measurements, and data analysis. M.I. and Y.H. contributed spectral measurements and analyzed obtained data. All authors read and approved the final manuscript.

Notes

The authors declare no competing financial interest.

■ ACKNOWLEDGMENTS

This work was supported by a Grant-in-Aid for Scientific Research (26400436) of the Japan Society for the Promotion of Science (JSPS).

■ ABBREVIATIONS

SWNTs, single-walled carbon nanotubes; NIR, near-infrared; PL, photoluminescence; H_2O_2, hydrogen peroxide

■ REFERENCES

(1) Krupke, R.; Hennrich, F.; Hampe, O.; Kappes, M. M. Near-infrared absorbance of single-walled carbon nanotubes dispersed in dimethylformamide. *J. Phys. Chem. B* **2003**, *107*, 5667−5669.

(2) Barone, P. W.; Baik, S.; Heller, D. A.; Strano, M. S. Near-infrared optical sensors based on single-walled carbon nanotubes. *Nat. Mater.* **2004**, *4*, 86−92.

(3) Palwai, N. R.; Martyn, D. E.; Neves, L. F. F.; Tan, Y.; Resasco, D. E.; Harrison, R. G. Retention of biological activity and near-infrared absorbance upon adsorption of horseradish peroxidase on single-walled carbon nanotubes. *Nanotechnology* **2007**, *18*, 235601.

(4) Xu, Y.; Pehrsson, P. E.; Chen, L.; Zhang, R.; Zhao, W. Double-stranded DNA single-walled carbon nanotube hybrids for optical hydrogen peroxide and glucose sensing. *J. Phys. Chem. C* **2007**, *111*, 8638−8643.

(5) Kono, J.; Ostojic, G. N.; Zaric, S.; Strano, M. S.; Moore, V. C.; Shaver, J.; Hauge, R. H.; Smalley, R. E. Ultra-fast optical spectroscopy of micelle-suspended single-walled carbon nanotubes. *Appl. Phys. A Mater. Sci. Process.* **2004**, *78*, 1093−1098.

(6) Kose, M. E.; Harruff, B. A.; Lin, Y.; Veca, L. M.; Lu, F.; Sun, Y.-P. Efficient quenching of photoluminescence from functionalized single-walled carbon nanotubes by nitroaromatic molecules. *J. Phys. Chem. B* **2006**, *110*, 14032−14034.

(7) Barone, P. W.; Yoon, H.; Ortiz-García, R.; Zhang, J.; Ahn, J.-H.; Kim, J.-H.; Strano, M. S. Modulation of Single-Walled Carbon Nanotube Photoluminescence by Hydrogel Swelling. *ACS Nano* **2009**, *3*, 3869−3877.

(8) Ju, S.-Y.; Kopcha, W. P.; Papadimitrakopoulos, F. Brightly Fluorescent Single-Walled Carbon Nanotubes via an Oxygen-Excluding Surfactant Organization. *Science* **2009**, *323*, 1319−1323.

(9) Liu, X.; Kuzmany, H.; Ayala, P.; Calvaresi, M.; Zerbetto, F.; Pichler, T. Selective Enhancement of Photoluminescence in Filled Single-Walled Carbon Nanotubes. *Adv. Funct. Mater.* **2012**, *22*, 3202−3208.

(10) Zhou, J.; Li, J.-p.; Nie, Y.-h.; Li, J.-s.; Yang, J.-f. Affinity and fluorescent detection of surfactants/ssDNA and single-walled carbon nanotube. *Trans. Nonferrous Met. Soc. China* **2013**, *23*, 456−461.

(11) Ito, M.; Ito, Y.; Nii, D.; Kato, H.; Umemura, K.; Homma, Y. The Effect of DNA Adsorption on Optical Transitions in Single Walled Carbon Nanotubes. *J. Phys. Chem. C* **2015**, *119*, 21141−21145.

(12) Lutsyk, P.; Piryatinski, Y.; AlAraimi, M.; Arif, R.; Shandura, M.; Kachkovsky, O.; Verbitsky, A.; Rozhin, A. Emergence of Additional Visible-Range Photoluminescence Due to Aggregation of Cyanine Dye: Astraphloxin on Carbon Nanotubes Dispersed with Anionic Surfactant. *J. Phys. Chem. C* **2016**, *120*, 20378−20386.

(13) Polo, E.; Kruss, S. Impact of Redox-Active Molecules on the Fluorescence of Polymer-Wrapped Carbon Nanotubes. *J. Phys. Chem. C* **2016**, *120*, 3061−3070.

(14) Rohringer, P.; Shi, L.; Ayala, P.; Pichler, T. Selective Enhancement of Inner Tube Photoluminescence in Filled Double-Walled Carbon Nanotubes. *Adv. Funct. Mater.* **2016**, *26*, 4874−4881.

(15) Shiraki, T.; Onitsuka, H.; Shiraishi, T.; Nakashima, N. Near infrared photoluminescence modulation of single-walled carbon nanotubes based on a molecular recognition approach. *Chem. Commun.* **2016**, *52*, 12972−12975.

(16) Hou, Z.; Krauss, T. D. Photoluminescence Brightening of Isolated Single-Walled Carbon Nanotubes. *J. Phys. Chem. Lett.* **2017**, *8*, 4954−4959.

(17) Jena, P. V.; Galassi, T. V.; Roxbury, D.; Heller, D. A. Review-Progress toward Applications of Carbon Nanotube Photoluminescence. *ECS J. Solid State Sci. Technol.* **2017**, *6*, M3075−M3077.

(18) Jena, P. V.; Safaee, M. M.; Heller, D. A.; Roxbury, D. DNA-Carbon Nanotube Complexation Affinity and Photoluminescence Modulation Are Independent. *ACS Appl. Mater. Interfaces* **2017**, *9*, 21397−21405.

(19) Carlson, L. J.; Krauss, T. D. Photophysics of individual single-walled carbon nanotubes. *Acc. Chem. Res.* **2008**, *41*, 235−243.

DOI: 10.1021/acsomega.9b00767
ACS Omega 2019, 4, 7750−7758

(20) Duque, J. G.; Cognet, L.; Parra-Vasquez, A. N. G.; Nicholas, N.; Schmidt, H. K.; Pasquali, M. Stable luminescence from individual carbon nanotubes in acidic, basic, and biological environments. *J. Am. Chem. Soc.* **2008**, *130*, 2626−2633.
(21) Welsher, K.; Liu, Z.; Daranciang, D.; Dai, H. Selective probing and imaging of cells with single walled carbon nanotubes as near-infrared fluorescent molecules. *Nano Lett.* **2008**, *8*, 586−590.
(22) Liu, Z.; Tabakman, S. M.; Chen, Z.; Dai, H. Preparation of carbon nanotube bioconjugates for biomedical applications. *Nat. Protoc.* **2009**, *4*, 1372−1381.
(23) Chen, Z.; Zhang, X.; Yang, R.; Zhu, Z.; Chen, Y.; Tan, W. Single-walled carbon nanotubes as optical materials for biosensing. *Nanoscale* **2011**, *3*, 1949−1956.
(24) Umemura, K. Hybrids of Nucleic Acids and Carbon Nanotubes for Nanobiotechnology. *Nanomaterials* **2015**, *5*, 321−350.
(25) Umemura, K.; Izumi, K.; Oura, S. Probe Microscopic Studies of DNA Molecules on Carbon Nanotubes. *Nanomaterials* **2016**, *6*, 180.
(26) Umemura, K.; Sato, S.; Bustamante, G.; Ye, J. Y. Using a fluorescence quenching method to detect DNA adsorption onto single-walled carbon nanotube surfaces. *Colloids Surf., B* **2017**, *160*, 201−206.
(27) Oura, S.; Umemura, K. Direct comparison of single- and multi-walled carbon nanotubes in fluorescence quenching phenomenon. *Jpn. J. Appl. Phys.* **2018**, *57*, 03EK04.
(28) Satishkumar, B. C.; Brown, L. O.; Gao, Y.; Wang, C.-C.; Wang, H.-L.; Doorn, S. K. Reversible fluorescence quenching in carbon nanotubes for biomolecular sensing. *Nat. Nanotechnol.* **2007**, *2*, 560−564.
(29) Homma, Y.; Hanashima, T.; Chiashi, S. Suspended Single-Wall Carbon Nanotubes as a Sensor of Molecular Adsorption. *Sens. Mater.* **2009**, *21*, 331−338.
(30) Jeng, E. S.; Nelson, J. D.; Prather, K. L. J.; Strano, M. S. Detection of a Single Nucleotide Polymorphism Using Single-Walled Carbon-Nanotube Near-Infrared Fluorescence. *Small* **2010**, *6*, 40−43.
(31) Kruss, S.; Hilmer, A. J.; Zhang, J.; Reuel, N. F.; Mu, B.; Strano, M. S. Carbon nanotubes as optical biomedical sensors. *Adv. Drug Deliv. Rev.* **2013**, *65*, 1933−1950.
(32) Wu, Z. L.; Gao, M. X.; Wang, T. T.; Wan, X. Y.; Zheng, L. L.; Huang, C. Z. A general quantitative pH sensor developed with dicyandiamide N-doped high quantum yield graphene quantum dots. *Nanoscale* **2014**, *6*, 3868−3874.
(33) Xu, S.; Liu, P.; Lu, X.; Zhang, J.; Huang, L.; Hua, W.; He, D.; Ouyang, J. A highly sensitive ″turn-on″ fluorescent sensor for the detection of human serum proteins based on the size exclusion of the polyacrylamide gel. *Electrophoresis* **2014**, *35*, 546−553.
(34) Kwon, H.; Kim, M.; Meany, B.; Piao, Y.; Powell, L. R.; Wang, Y. Optical Probing of Local pH and Temperature in Complex Fluids with Covalently Functionalized, Semiconducting Carbon Nanotubes. *J. Phys. Chem. C* **2015**, *119*, 3733−3739.
(35) Ko, Y.-I.; Kang, C.-S.; Shin, E.-A.; Jung, Y. C.; Muramatsu, H.; Hayashi, T.; Kim, Y. A.; Dresselhaus, M. S. Optical sensitivity of mussel protein-coated double-walled carbon nanotubes on the iron-DOPA conjugation bond. *RSC Adv.* **2016**, *6*, 16308−16313.
(36) Budhathoki-Uprety, J.; Langenbacher, R. E.; Jena, P. V.; Roxbury, D.; Heller, D. A. A Carbon Nanotube Optical Sensor Reports Nuclear Entry via a Noncanonical Pathway. *ACS Nano* **2017**, *11*, 3875−3882.
(37) Farrera, C.; Torres Andón, F.; Feliu, N. Carbon Nanotubes as Optical Sensors in Biomedicine. *ACS Nano* **2017**, *11*, 10637−10643.
(38) Kurnosov, N. V.; Karachevtsev, M. V.; Leontiev, V. S.; Karachevtsev, V. A. Tuning the carbon nanotube photoluminescence enhancement at addition of cysteine through the change of external conditions. *Mater. Chem. Phys.* **2017**, *186*, 131−137.
(39) Pan, J.; Li, F.; Choi, J. H. Single-walled carbon nanotubes as optical probes for bio-sensing and imaging. *J. Mater. Chem. B* **2017**, *5*, 6511−6522.
(40) Zhao, E. H.; Ergul, B.; Zhao, W. Caffeine's Antioxidant Potency Optically Sensed with Double-Stranded DNA-Encased Single-Walled Carbon Nanotubes. *J. Phys. Chem. B* **2015**, *119*, 4068−4075.
(41) Zhang, J.; Kruss, S.; Hilmer, A. J.; Shimizu, S.; Schmois, Z.; De La Cruz, F.; Barone, P. W.; Reuel, N. F.; Heller, D. A.; Strano, M. S. A Rapid, Direct, Quantitative, and Label-Free Detector of Cardiac Biomarker Troponin T Using Near-Infrared Fluorescent Single-Walled Carbon Nanotube Sensors. *Adv. Healthc. Mater.* **2014**, *3*, 412−423.
(42) Salem, D. P.; Landry, M. P.; Bisker, G.; Ahn, J.; Kruss, S.; Strano, M. S. Chirality dependent corona phase molecular recognition of DNA-wrapped carbon nanotubes. *Carbon* **2016**, *97*, 147−153.
(43) Landry, M. P.; Ando, H.; Chen, A. Y.; Cao, J.; Kottadiel, V. I.; Chio, L.; Yang, D.; Dong, J.; Lu, T. K.; Strano, M. S. Single-molecule detection of protein efflux from microorganisms using fluorescent single-walled carbon nanotube sensor arrays. *Nat. Nanotechnol.* **2017**, *12*, 368−377.
(44) Giraldo, J. P.; Landry, M. P.; Kwak, S.-Y.; Jain, R. M.; Wong, M. H.; Iverson, N. M.; Ben-Naim, M.; Strano, M. S. A Ratiometric Sensor Using Single Chirality Near-Infrared Fluorescent Carbon Nanotubes: Application to In Vivo Monitoring. *Small* **2015**, *11*, 3973−3984.
(45) Bisker, G.; Dong, J.; Park, H. D.; Iverson, N. M.; Ahn, J.; Nelson, J. T.; Landry, M. P.; Kruss, S.; Strano, M. S. Protein-targeted corona phase molecular recognition. *Nat. Commun.* **2016**, *7*, 10241.
(46) Agrawal, K. V.; Drahushuk, L. W.; Strano, M. S. Observation and analysis of the Coulter effect through carbon nanotube and graphene nanopores. *Philos. Trans. R. Soc. A-Math. Phys. Eng. Sci.* **2016**, *374*, 20150357.
(47) Tu, X.; Pehrsson, P. E.; Zhao, W. Redox reaction of DNA-Encased HiPco carbon nanotubes with hydrogen peroxide: A near infrared optical sensitivity and kinetics study. *J. Phys. Chem. C* **2007**, *111*, 17227−17231.
(48) Kruss, S.; Landry, M. P.; Vander Ende, E.; Lima, B. M. A.; Reuel, N. F.; Zhang, J.; Nelson, J.; Mu, B.; Hilmer, A.; Strano, M. Neurotransmitter Detection Using Corona Phase Molecular Recognition on Fluorescent Single-Walled Carbon Nanotube Sensors. *J. Am. Chem. Soc.* **2014**, *136*, 713−724.
(49) Meyer, D.; Hagemann, A.; Kruss, S. Kinetic Requirements for Spatiotemporal Chemical Imaging with Fluorescent Nanosensors. *ACS Nano* **2017**, *11*, 4017−4027.
(50) Yudasaka, M.; Yomogida, Y.; Zhang, M. F.; Tanaka, T.; Nakahara, M.; Kobayashi, N.; Okamatsu-Ogura, Y.; Machida, K.; Ishihara, K.; Saeki, K.; Kataura, H. Near-Infrared Photoluminescent Carbon Nanotubes for Imaging of Brown Fat. *Sci. Rep.* **2017**, *7*, 44760.
(51) Shearer, C. J.; Yu, L.; Fenati, R.; Sibley, A. J.; Quinton, J. S.; Gibson, C. T.; Ellis, A. V.; Andersson, G. G.; Shapter, J. G. Adsorption and Desorption of Single-Stranded DNA from Single-Walled Carbon Nanotubes. *Chem.—Asian J.* **2017**, *12*, 1625−1634.
(52) Ishihara, S.; O'Kelly, C. J.; Tanaka, T.; Kataura, H.; Labuta, J.; Shingaya, Y.; Nakayama, T.; Ohsawa, T.; Nakanishi, T.; Swager, T. M. Metallic versus Semiconducting SWCNT Chemiresistors: A Case for Separated SWCNTs Wrapped by a Metallosupramolecular Polymer. *ACS Appl. Mater. Interfaces* **2017**, *9*, 38062−38067.
(53) Ishibashi, Y.; Ito, M.; Homma, Y.; Umemura, K. Monitoring the antioxidant effects of catechin using single-walled carbon nanotubes: Comparative analysis by near-infrared absorption and near-infrared photoluminescence. *Colloids Surf., B* **2018**, *161*, 139−146.
(54) Weisman, R. B.; Bachilo, S. M. Dependence of optical transition energies on structure for single-walled carbon nanotubes in aqueous suspension: An empirical Kataura plot. *Nano Lett.* **2003**, *3*, 1235−1238.
(55) Kato, Y.; Inoue, A.; Niidome, Y.; Nakashima, N. Thermodynamics on Soluble Carbon Nanotubes: How Do DNA Molecules Replace Surfactants on Carbon Nanotubes? *Sci. Rep.* **2012**, *2*, 733.
(56) Yoshikawa, K.; Matsunaga, R.; Matsuda, K.; Kanemitsu, Y. Mechanism of exciton dephasing in a single carbon nanotube studied by photoluminescence spectroscopy. *Appl. Phys. Lett.* **2009**, *94*, 093109.
(57) Stich, D.; Späth, F.; Kraus, H.; Sperlich, A.; Dyakonov, V.; Hertel, T. Triplet-triplet exciton dynamics in single-walled carbon nanotubes. *Nat. Photonics* **2014**, *8*, 139−144.

DOI: 10.1021/acsomega.9b00767
ACS Omega 2019, 4, 7750−7758

(58) Rajan, A.; Strano, M. S.; Heller, D. A.; Hertel, T.; Schulten, K. Length-Dependent Optical Effects in Single Walled Carbon Nanotubes. *J. Phys. Chem. B* **2008**, *112*, 6211−6213.
(59) Qian, Z.; Zhou, J.; Ma, J.; Shan, X.; Chen, C.; Chen, J.; Feng, H. The visible photoluminescence mechanism of oxidized multi-walled carbon nanotubes: an experimental and theoretical investigation. *J. Mater. Chem. C* **2013**, *1*, 307−314.
(60) Lutsyk, P.; Arif, R.; Hruby, J.; Bukivskyi, A.; Vinijchuk, O.; Shandura, M.; Yakubovskyi, V.; Kovtun, Y.; Rance, G. A.; Fay, M.; Piryatinski, Y.; Kachkovsky, O.; Verbitsky, A.; Rozhin, A. A sensing mechanism for the detection of carbon nanotubes using selective photoluminescent probes based on ionic complexes with organic dyes. *Light Sci. Appl.* **2016**, *5*, No. e16028.
(61) Lefebvre, J.; Maruyama, S.; Finnie, P. Photoluminescence: Science and applications. In *Carbon Nanotubes: Advanced Topics in the Synthesis, Structure, Properties and Applications*; Jorio, A., Dresselhaus, G., Dresselhaus, M. S., Eds.; Springer-Verlag Berlin: Berlin, 2008; Vol. *111*, pp 287−319.
(62) Carlson, L. J.; Maccagnano, S. E.; Zheng, M.; Silcox, J.; Krauss, T. D. Fluorescence efficiency of individual carbon nanotubes. *Nano Lett.* **2007**, *7*, 3698−3703.
(63) Budhathoki-Uprety, J.; Jena, P. V.; Roxbury, D.; Heller, D. A. Helical Polycarbodiimide Cloaking of Carbon Nanotubes Enables Inter-Nanotube Exciton Energy Transfer Modulation. *J. Am. Chem. Soc.* **2014**, *136*, 15545−15550.
(64) Baranowska, M.; Suliborska, K.; Chrzanowski, W.; Kusznierewicz, B.; Namieśnik, J.; Bartoszek, A. The relationship between standard reduction potentials of catechins and biological activities involved in redox control. *Redox Biol.* **2018**, *17*, 355−366.
(65) Hirana, Y.; Juhasz, G.; Miyauchi, Y.; Mouri, S.; Matsuda, K.; Nakashima, N. Empirical Prediction of Electronic Potentials of Single-Walled Carbon Nanotubes With a Specific Chirality (n,m). *Sci. Rep.* **2013**, *3*, 2959.
(66) Tanaka, Y.; Hirana, Y.; Niidome, Y.; Kato, K.; Saito, S.; Nakashima, N. Experimentally Determined Redox Potentials of Individual (n,m) Single-Walled Carbon Nanotubes. *Angew. Chem., Int. Ed.* **2009**, *48*, 7655−7659.

DOI: 10.1021/acsomega.9b00767
ACS Omega 2019, 4, 7750−7758